Journal of Thermal Analysis, Vol. 54 (1998) 623-635

TEMPERATURE MODULATED DSC OF IRREVERSIBLE MELTING OF NYLON 6 CRYSTALS

A. Toda, C. Tomita and M. Hikosaka*

Faculty of Integrated Arts and Sciences, Hiroshima University, 1-7-1 Kagamiyama
Higashi-Hiroshima 739-8521, Japan

Abstract

A new method is presented to analyze the irreversible melting kinetics of polymer crystals with a temperature modulated differential scanning calorimetry (TMDSC). The method is based on an expression of the apparent heat capacity, $\Delta\tilde{C}e^{-i\alpha}=mc_p+i(1/\omega)F\dagger$, with the true heat capacity, mc_p, and the response of the kinetics, $F\dagger$. The present paper experimentally examines the irreversible melting of nylon 6 crystals on heating. The real and imaginary parts of the apparent heat capacity showed a strong dependence on frequency and heating rate during the melting process. The dependence and the Cole-Cole plot could be fitted by the frequency response function of Debye's type with a characteristic time depending on heating rate. The characteristic time represents the time required for the melting of small crystallites which form the aggregates of polymer crystals. The heating rate dependence of the characteristic time differentiates the superheating dependence of the melting rate. Taking account of the relatively insensitive nature of crystallization to temperature modulation, it is argued that the 'reversing' heat flow extrapolated to $\omega \to 0$ is related to the endothermic heat flow of melting and the corresponding 'non-reversing' heat flow represents the exothermic heat flow of re-crystallization and re-organization. The extrapolated 'reversing' and 'non-reversing' heat flow indicates the melting and re-crystallization and/or re-organization of nylon 6 crystals at much lower temperature than the melting peak seen in the total heat flow.

Keywords: kinetics of melting, polymer crystals, temperature-modulated DSC

Introduction

We have recently proposed a new analyzing method of Temperature Modulated DSC (TMDSC) [1–6] applicable to irreversible transformation kinetics such as polymer crystallization [7–10] and melting [11, 12]. The analysis is based on the behaviour of an apparent heat capacity of complex quantity, $\Delta\tilde{C}e^{-i\alpha}\equiv\Delta\tilde{C}'-i\Delta\tilde{C}''$, determined from the modulation amplitude and phase angle of sample temperature, $T_s=\bar{T}_s+\tilde{T}_se^{i(\omega t+\varepsilon)}$ and heat flow, $Q=\bar{Q}+\tilde{Q}e^{i(\omega t+\delta)}$, as,

$$\tilde{Q}e^{i(\omega t+\delta)}=-\Delta\tilde{C}e^{-i\alpha}\frac{d}{dt}\tilde{T}_se^{i(\omega t+\varepsilon)} \quad (1)$$

* Author for correspondence, tel: +81-(0)824-24-6558, fax: +81-(0)824-24-0757,
Email: atoda@ipc.hiroshima-u.ac.jp

1418–2874/98/ $ 5.00

Akadémiai Kiadó, Budapest
Kluwer Academic Publishers, Dordrecht

$$\frac{\tilde{Q}}{\omega \tilde{T}_s} \rightarrow \Delta \tilde{C} \tag{2}$$

$$\alpha \equiv (\varepsilon - \delta) - (\varepsilon - \delta)_0 \tag{3}$$

where $(\varepsilon-\delta)_0$ represents the baseline of the difference in the phase angle and the arrow in Eq. (2) means that a calibration is required. For the irreversible transformation processes of crystallization and melting, we have proposed the following expression of the apparent heat capacity,

$$\Delta \tilde{C} e^{-i\alpha} = mc_p + i\frac{1}{\omega}F'_T \tag{4}$$

where mc_p is the true heat capacity of sample and F'_T represents the temperature derivative of the kinetic response.

The true heat capacity, mc_p, can be frequency dependent and undergoes a relaxation process such as α process related to the glass transition giving a negative imaginary part as a consequence of irreversibility [13, 14]. The coefficient F'_T can also be of complex quantity, depending on the frequency response of kinetics to temperature modulation. In the case of polymer crystallization, the apparent heat capacity showed a frequency response indicating a constant F'_T independent of frequency [9, 10]. The irreversible melting of polymer crystals on heating, on the other hand, showed a quite strong dependence on frequency of the real and imaginary parts of the apparent heat capacity, indicating that the characteristic time of the melting is comparable with the applied modulation period [11, 12]. The frequency dependence could be approximated as,

$$\Delta \tilde{C} e^{-i\alpha} \approx C + \frac{D}{1 + i\omega\tau(\beta)} \tag{5}$$

where C and D are constants and the characteristic time, $\tau(\beta)$, depends on the heating rate, β, as,

$$\tau \propto \beta^x \quad \text{with} \quad -1 \leq x \leq 0 \tag{6}$$

($-1<x<-0.5$ for poly(ethylene terephthalate) (PET) [11] and $-0.5<x<0$ for polyethylene [12]).

Polymer crystals should be considered as the aggregates of small crystallites having a continuous distribution of the non-equilibrium melting points determined mainly by the distributions of lamellar thickness and of molecular mass. Therefore, the characteristic time of melting should be of the small crystallites. We have found that τ shows a temperature dependence, suggesting shorter τ at lower temperatures; the result will be expected for the less stable crystallites having lower melting temperature.

In the preceding papers [11, 12], we have modeled the irreversible melting of crystallites on heating by introducing the fraction of the crystallites, $\varphi(t,T_m)dT_m$, having the melting temperature in the range from T_m to T_m+dT_m. The change in the fraction is given by the melting rate coefficient, R, as $\varphi(\Delta t,T_m)=\varphi(0,T_m)\exp\left[-\int_0^{\Delta t}R\,dt'\right]$. The total melting rate is then represented by the time derivative of the total crystallinity, $\Phi(t)$, expressed as, $\Phi(t)=\int_0^{\infty}dT_m\varphi(t,T_m)$, and hence the endothermic heat flow of melting, $F_{melt}(t)$, is given as $F_{melt}(t)=\Delta H(d\Phi/dt)$. In order to calculate the steady response of the melting kinetics, we assumed a hypothetical situation of uniform distribution of the initial fractions, $\varphi(0,T_m)=\varphi_o$. This assumption can be applied if the actual melting points have a distribution wide enough compared to the modulation period and to the characteristic time of the melting of crystallites. The condition is represented as follows,

$$\text{(Temperature range in which the change in } \varphi_o(T_m) \text{ is negligible)} \quad (7)$$

$$>> \beta \times \text{ (period of modulation)}$$

and

$$>> 2\pi\beta\tau \quad (8)$$

For the uniform distribution, the kinetic response is represented by a Fourier series expressed as,

$$F_{melt}(t) = \bar{F}_{melt} + F'_T(\omega)\tilde{T}_s e^{i\omega t} + \ldots \quad (9)$$

$$\bar{F}_{melt} = -\beta\Delta H\varphi_o \quad (10)$$

$$F'_T(\omega)\tilde{T}_s = \beta\varphi_o\int_{-\infty}^{\infty}e^{-i\omega t}F_{melt}(t)dt \quad (11)$$

Here, the contribution of the kinetic response to the apparent heat capacity is given by $(i/\omega)F'_T(\omega)$ as shown in Eq. (4).

We have examined three different dependences on superheating, ΔT, of the melting rate coefficient, $R(\Delta T)$: constant K_o, linear dependence on superheating of $R_1=a\Delta T$ and exponential dependence of $R_2\propto e^{c\Delta T}$. In order to calculate the Fourier integral of Eq. (11) with those dependences, we have applied the expansion of $R(\Delta T)$ in terms of modulation component, $\tilde{T}_s e^{i(\omega t+\varepsilon)}$, as follows,

$$\Delta T = \beta\Delta t + \tilde{T}_s e^{i\omega t_0}\left(e^{i\omega\Delta t} - 1\right) \tag{12}$$

$$R(\Delta T) = R(\beta\Delta t) + R'(\beta\Delta t)\tilde{T}_s e^{i\omega t_0}\left(e^{i\omega\Delta t} - 1\right) + \ldots \tag{13}$$

where $\Delta t \equiv t - t_0$ and t_0 means the time when the melting of the fraction begins. In the analysis [11, 12], we employed the expansion up to the first order because we are concerned with the first harmonic of Eq. (9). With the expansion, the frequency response of the apparent heat capacity in Eq. (4) has been calculated. The calculated results can be approximated by the following formula,

$$\Delta\tilde{C}e^{-i\alpha} = mc_p + \frac{(-\bar{F}_{melt}/\beta)}{1 + i\omega\tau(\beta)} \tag{14}$$

where the heating rate dependence of $\tau(\beta)$ becomes as $\tau_0 \equiv 1/R_0$ for R_0, $\tau_1 \equiv 1/(2a\beta)^{1/2}$ for R_1 and $\tau_2 \equiv 1/(\beta c)$ for R_2; the dependence is in the range of Eq. (6) and is determined by the superheating dependence of $R(\Delta T)$.

In summary, TMDSC is applicable to the melting process having a temperature distribution wide enough. Firstly, by examining the frequency dependence of the apparent heat capacity during the melting process, we are able to discuss the characteristic time of the melting of crystallites. Secondly, from the heating rate dependence of the characteristic time, we can differentiate the superheating dependence of the melting rate coefficient. Those information will be quite valuable for the investigation of the melting process, because we are not able to observe the melting process of small crystallites directly by microscopy.

Concerned with the melting of polymer crystals [15], it is also well known that the melting of polymer crystallites is followed by subsequent re-crystallization. Re-organization of the remaining crystallites also sets in for the temperature range of the melting. Those processes complicate the interpretation of the melting process. Since they are exothermic, the total heat flow, Q, is the sum of the endothermic heat flow of melting, $F_{melt}<0$, the exothermic heat flow of re-crystallization and re-organization, $F_{exo}>0$, and the contribution of the heat capacity, $-\beta mc_p$, represented as,

$$\dot{Q} = -\beta mc_p + F_{melt} + F_{exo} \tag{15}$$

The response to temperature modulation is therefore composed of the response of those three contributions schematically described in Fig. 1. As is shown in Fig. 2 in the case of nylon 6 crystals, it has been confirmed that the response of crystallization appearing in the apparent heat capacity is much smaller than that of melting process. In Fig. 1, the response appears as the modulation of each heat flow, and the modulation of the exothermic heat flow of crystallization is drawn negligibly smaller than the others. Since the apparent heat capacity is determined by the modulation, we can neglect the response of re-crystallization and re-organization in the apparent heat capacity and we employ the expression

of the apparent heat capacity of Eq. (14) in which only the melting process is considered. Concerned with the mean 'total' heat flow, $\bar{Q}$, on the other hand, the mean exothermic heat flow, F_{exo}, due to re-crystallization and re-organization contributes in a considerable amount. If we can utilize the expression of the apparent heat capacity given by Eq. (14), we can obtain the mean endothermic heat flow, $-\beta mc_p+F_{melt}$, from the extrapolation of the 'reversing' heat flow, $-\beta\Delta\tilde{C}(\omega \rightarrow 0)$. The mean exothermic heat flow, F_{exo}, is then evaluated by the extrapolated 'non-reversing' heat flow, $\bar{Q}-[-\beta\Delta\tilde{C}(\omega \rightarrow 0)]$. Therefore, the 'reversing' and 'non-reversing' heat flow extrapolated to $\omega \rightarrow 0$ has the strict physical meaning. The extrapolation of the 'reversing' heat flow to the opposite $\omega \rightarrow \infty$ gives us the true heat capacity, mc_p, during the melting process. We are able to understand the complicated behaviours of the melting, re-crystallization and re-organization, by applying this separation.

Experimentally, we have applied this separation method to PET [11] and polyethylene [12]; PET is known to exhibit quite large re-crystallization and/or re-organization, while in polyethylene the effect is not significant if the sample is crystallized by slow cooling [15, 16]. In the case of PET, the extrapolated $-\beta\Delta\tilde{C}(\omega \rightarrow 0)$ was actually much larger than the total heat flow, $\bar{Q}$, indicating the exothermic heat flow of re-crystallization and/or re-organization. For polyethylene, on the other hand, re-crystallization and/or re-organization is much smaller and the relation $\bar{Q}=-\beta\Delta\tilde{C}(\omega \rightarrow 0)$ has been confirmed experimentally for the samples prepared by slow cooling.

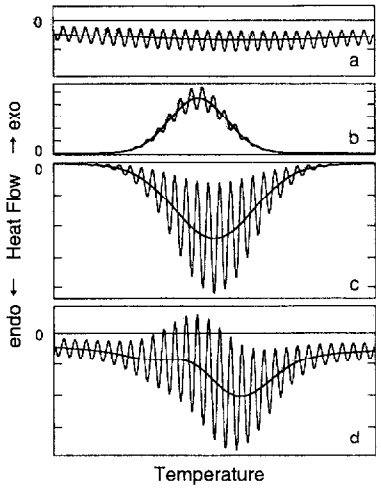

Fig. 1 Schematic representation of the components of modulated heat flow: (a) contribution of the true heat capacity, $-\beta mc_p$, (b) exothermic heat flow of re-crystallization and re-organization, F_{exo}, (c) endothermic heat flow of melting, F_{melt}, and (d) the total heat flow, $\bar{Q}$, obtained by the sum. Though the mean exothermic heat flow of re-crystallization and re-organization is appreciable, the modulation amplitude is expected to be much smaller than that of melting

In the present paper, we examine the irreversible melting of nylon 6 crystals on heating. The melting of nylon 6 crystals as well as of PET is known to be followed by re-crystallization and/or re-organization and the melting of the original crystallites begins at much lower temperature than the melting peak observed in the total heat flow [17]. We analyze the melting behaviour with the new analysis method explained above.

Experimental

The DSC 2920 Module controlled with Thermal Analyst 2200 (TA Instruments) was used for all measurements. Nitrogen gas with a flow rate of 40 ml min^{-1} was purged through the cell. The DSC runs consisted of cyclic heating and cooling with different modulation periods and heating rates for a single sample of nylon 6 (poly(caprolactam), Scientific Polymer Products, Inc.) the mass of which was 3.50 mg. The crystallization was provided by a cooling run at the rate of 20 K min^{-1} from the melt kept at 245°C. The starting temperature of

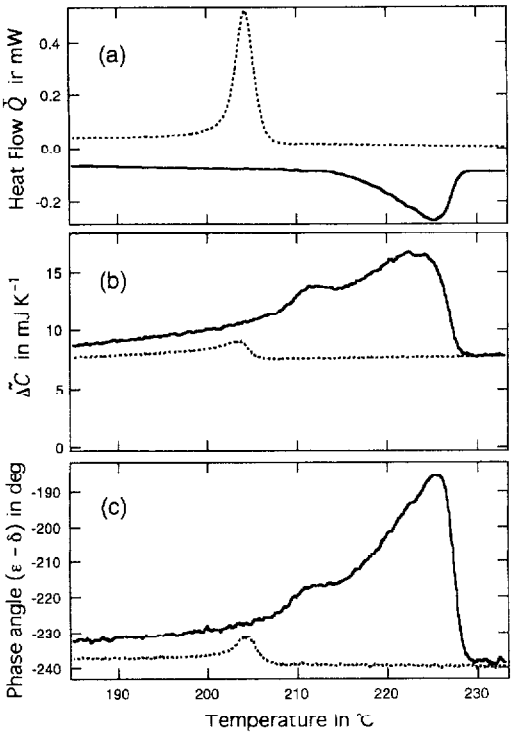

Fig. 2 Raw data of TMDSC on heating (solid lines, melting) and cooling (broken lines, crystallization) of nylon 6 at the rate of 0.4 K min^{-1}: (a) total heat flow $\bar{Q}$. (b) the magnitude of the apparent heat capacity $\Delta\tilde{C}$ and (c) phase angle (ε–δ). The modulation periods are of 68 s

heating runs was 100°C and the heating rate was in the range of 0.4–4.5 K min^{-1}. The modulation period of 28–100 s was examined with the modulation amplitude satisfying the heating only condition of $dT_s/dt>0$ ($\tilde{T}_s<\beta/\omega$). The apparent heat capacity of each run with different modulation periods was normalized by the value of the melt at 233°C and hence the apparent heat capacity has been automatically calibrated for different modulation periods. The baseline of the phase lag, $(\varepsilon-\delta)_0$, was assumed to be a straight line connecting the temperature range outside the melting region.

Results and discussion

Figure 3 shows the typical data of (a) total heat flow, $\dot{Q}$, (b) normalized magnitude of the apparent heat capacity, $\Delta\tilde{C}$, and (c) the difference in phase angle, $(\varepsilon-\delta)$, for different periods of modulation. It is noted that the change in the magnitude and phase angle is seen at much lower temperature than the melting peak

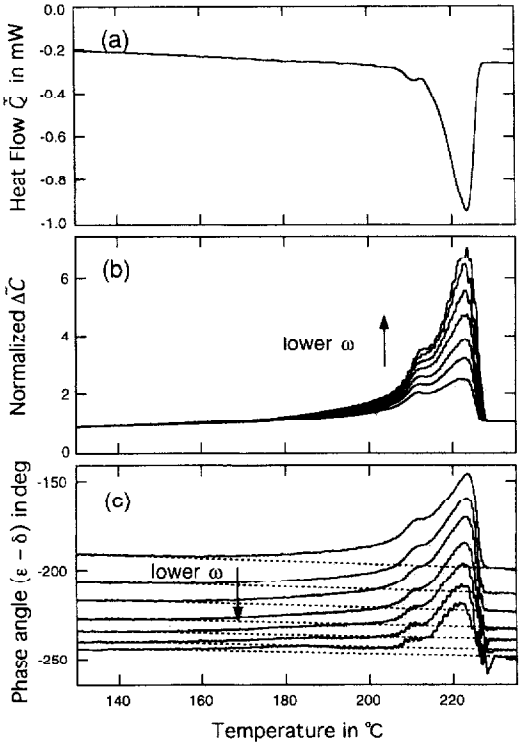

Fig. 3 Raw data of TMDSC showing the frequency dependence of the melting process of nylon 6 crystals by heating runs at 1.6 K min^{-1}: (a) total heat flow $\bar{Q}$, (b) the magnitude of the apparent heat capacity $\Delta\tilde{C}$ normalized by the value of the melt at 233°C and (c) phase angle $(\varepsilon-\delta)$. The modulation periods are of 28, 36, 44, 56, 68, 84 and 100 s. In (c), the dotted lines represent the baseline, $(\varepsilon-\delta)_0$

in the total heat flow. This change indicates the beginning of the melting at much lower temperature than the apparent melting peak in the total heat flow, which is the sum of the endothermic heat flow of melting and the exothermic heat flow of re-crystallization and re-organization; the melting at lower temperature has been confirmed experimentally by Todoki *et al.* [17].

The base-line of the phase angle, $(\varepsilon-\delta)_o$, was taken as a straight dotted line shown in Fig. 3c for each modulation period. Since the magnitude in Fig. 3b is normalized, the necessary calibration of Eq. (2) has been automatically taken into account, except for the dependence of the calibration constant on the sample heat capacity itself. The correction term due to the sample heat capacity is proportional to the sample heat capacity and inversely proportional to modulation period. For the modulation period applied in the present experiments (28–100 s), we are able to neglect the correction with the apparent heat capacity of the present sample less than 40 mJ K^{-1}. The details of the correction will be discussed in a forthcoming paper.

Normalized real and imaginary parts of the apparent heat capacity were calculated from the data and shown in Fig. 4. It is clearly seen that both of the real and imaginary parts show strong dependence on modulation frequency.

Figure 5 shows the frequency dependence and Cole-Cole plot of the real and imaginary parts at the same temperature of 215.0°C for several different heating rates. The curved lines in Fig. 5 are the frequency response function of Debye's type given by Eq. (14). The fitting to Eq. (14) was done with the adjustable parameters of mc_p, $F_{melt}(\varphi_o)$ and τ. In Fig. 5, we can see that the behaviour in the frequency dependence has a strong dependence on heating rate. It should also be noted that the deviation from the fitting curve becomes appreciable for longer modulation

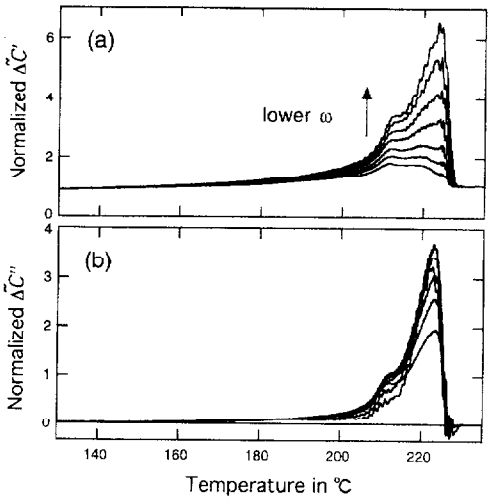

Fig. 4 Frequency dependence of (a) the real part $\Delta\tilde{C}'$ and (b) the imaginary part $\Delta\tilde{C}''$ of the apparent heat capacity obtained by the data shown in Fig. 3

period (lower frequency) at higher heating rate. One reason for this deviation is that the number of modulation periods in the melting peak becomes smaller for longer modulation period at higher heating rate; the requirement of Eq. (7) was not satisfied under the condition. When the condition is not satisfied, the melting process cannot be in quasi-steady state. By plotting Lissajous diagram of the modulated heat flow *vs.* modulated sample temperature, we can see whether the steady response is attained [18,19]. In Fig. 6, two cycles of Lissajous diagram are plotted and we can see that, for longer modulation period at higher heating rate, the response is not in quasi-steady state.

Concerned with non-linear response, the overall shape of Lissajous diagram should be an ellipse if the response is linear; hence the departure from an ellipse in Fig. 6 indicates a non-linear response of the melting kinetics. The non-linearity is also indicated by taking the ratio of the second harmonic and the first har-

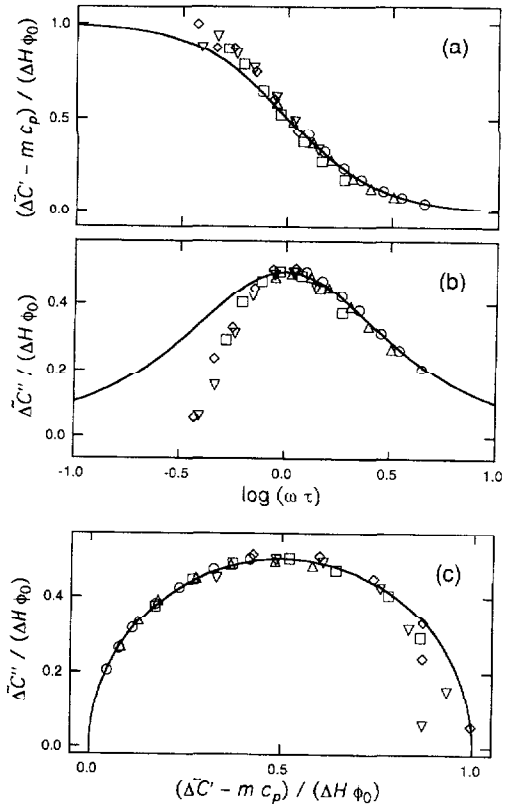

Fig. 5 Plots of the (a) real and (b) imaginary parts of the normalized apparent heat capacity during the melting process of nylon 6 *vs.* modulation frequency. Cole-Cole plots of the data is shown in (c).
The data at 215.0°C were taken from the heating runs of the following rates: 0.4 (○), 0.8 (△), 1.6 (□), 3.2 (▽) and 4.5 K min^{-1} (◇). The curved lines are the plots of Eq. (14) with the adjustable parameters of c_p, $\bar{F}_{melt}(\varphi_o)$ and τ

monic of modulated heat flow, which amounts to several % in the melting peak. From those evidences of Lissajous diagram and the appreciable amount of the second harmonic, it is experimentally obvious that the response in heat flow has higher harmonics. Therefore, the nonlinearity is not negligible in the melting process. In order to fully understand the response of heat flow during the melting process, the analysis must be based on the non-linearity of the response. Our model actually predicts higher harmonics in the response [11, 12] and hence the model is capable of incorporating the non-linear response of melting kinetics if the higher order expansion is considered in Eq. (13); numerical calculations based on the model will be presented separately. The purpose of the present paper is to show that the first harmonic contains quite valuable information such as the

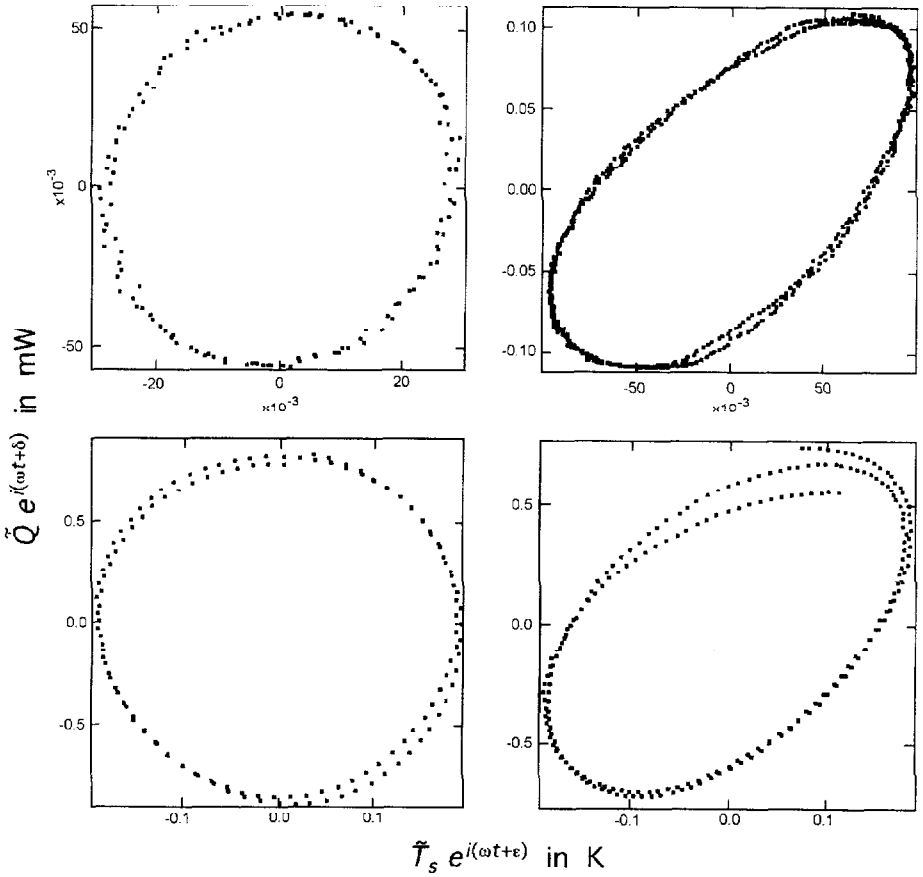

Fig. 6 Lissajous diagrams of the modulation component of heat flow during the melting peak plotted against that of sample temperature. The two cycles of the modulation are plotted. The heating rate and the modulation period of TMDSC are the followings: (a) 0.4 K min^{-1} and 28 s, (b) 0.4 K min^{-1} and 100 s, (c) 4.5 K min^{-1} and 28 s and (d) 4.5 K min^{-1} and 44 s

characteristic time of melting and hence we employed the expansion only up to the first order in Eq. (13).

Figure 7 shows the dependence on temperature and on heating rate of the characteristic time determined by the fitting such as shown in Fig. 5. In the case of nylon 6, the temperature dependence does not show the systematic change observed for the melting of PET and polyethylene crystals. The heating rate dependence, on the other hand, could be approximated as $\tau \propto \beta^{-0.5}$ and indicates the linear dependence on superheating of the melting rate coefficient. For the melting of polymer crystals, we expect an exponential dependence on superheating of the melting rate [16]. Since the exponential dependence can be approximated by the linear dependence for superheating small enough, the linear dependence means that the melting completes at lower superheating compared to the case of the exponential dependence. The exponential dependence corresponds to the case of $\tau \propto \beta^{-1}$ and has been confirmed in the melting of PET crystals [11]. Utilizing this analysis, we can therefore differentiate the melting processes of different polymers.

Figure 8 shows the extrapolated 'reversing' heat flow representing $-\beta\Delta\bar{C}(\omega \rightarrow 0) = -\beta mc_p + \bar{F}_{melt}$. The 'reversing' heat flow is much larger than the total heat flow, $\dot{Q}$, because of the exothermic heat flow of re-crystallization and/or

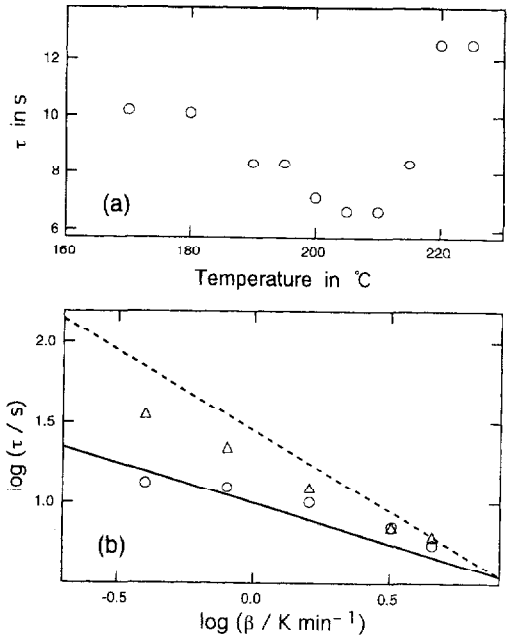

Fig. 7 Plots of the characteristic time τ chosen for the fitting such as shown in Fig. 5 *vs.* (a) temperature and (b) heating rate, β. In (a) the values were determined for the heating rate of 1.6 K min^{-1} and, in (b), the symbols represent the values for the temperatures of 180.0 (○) and 220.0°C (△). The slopes of the solid and broken lines in (b) are –0.5 and –1, respectively

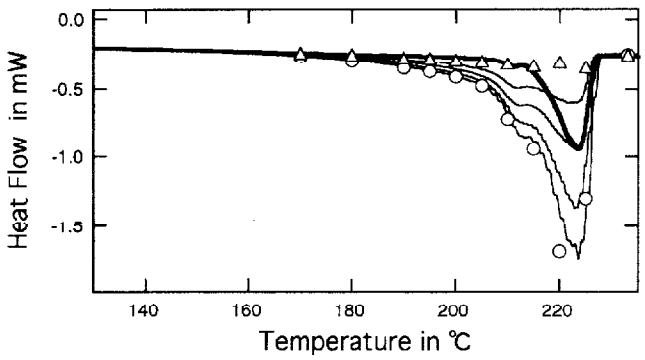

Fig. 8 Plots of the 'total' heat flow $\overline{Q}$ (thick line) and the 'reversing' heat flow (thin lines) obtained with the modulation periods of 28–100 s for the heating rate of 1.6 K min^{-1}. Symbols represent the 'reversing' heat flow extrapolated to $\omega \rightarrow 0$, $-\beta mc_p+F_{melt}$, (o) and the contribution of the true heat capacity, $-\beta mc_p$ (Δ) determined by the fitting to Eq. (14) of the apparent heat capacity, respectively

re-organization in $\overline{Q}$. The difference between the extrapolated 'reversing' heat flow and the total heat flow gives the extrapolated 'non-reversing' heat flow representing F_{exo}. It is clearly seen that the melting (and re-crystallization and/or re-organization) starts at much lower temperature than the melting peak appearing in the total heat flow.

Conclusion

The irreversible melting behaviour of nylon 6 crystals has been analyzed by the new method of TMDSC. The characteristic time of the melting of crystallites has been obtained from the frequency dependence of the apparent heat capacity. The heating rate dependence of the characteristic time, $\tau \propto \beta^{-0.5}$, indicates the linear dependence of the melting rate coefficient on superheating. By extrapolating the 'reversing' and 'non-reversing' heat flow to $\omega \rightarrow 0$, the separation of the melting and re-crystallization and/or re-organization has been done and the results suggest the beginning of those processes at much lower temperature than the melting peak in the total heat flow. By examining those characteristics for many other polymers, we will be able to classify the melting of polymer crystals by their behaviours obtained by TMDSC.

References

1 P. S. Gill, S. R. Sauerbrunn and M. Reading, J. Thermal Anal., 40 (1993) 931.
2 M. Reading, D. Elliott and V. L. Hill, J. Thermal Anal., 40 (1993) 949.
3 M. Reading, A. Luget and R. Wilson, Thermochim. Acta, 238 (1994) 295.
4 B. Wunderlich, Y. Jin and A. Boller, Thermochim. Acta, 238 (1994) 277.
5 A. Boller, Y. Jin and B. Wunderlich, J. Thermal Anal., 42 (1994) 307.

6 I. Hatta, Jpn. J. Appl. Phys., 33 (1994) L686.
7 A. Toda, T. Oda, M. Hikosaka and Y. Saruyama, Polymer, 38 (1997) 231.
8 A. Toda, T. Oda, M. Hikosaka and Y. Saruyama, Thermochim. Acta, 293 (1997) 47.
9 A. Toda, C. Tomita, M. Hikosaka and Y. Saruyama, Polymer, 38 (1997) 2849.
10 A. Toda, C. Tomita, M. Hikosaka and Y. Saruyama, Polymer, 39 (1998) 1439.
11 A. Toda, C. Tomita, M. Hikosaka and Y. Saruyama, Polymer, 39 (1998) 5093.
12 A. Toda, C. Tomita, M. Hikosaka and Y. Saruyama, Thermochim. Acta, in press.
13 N. O. Birge and S. R. Nagel, Phys. Rev. Lett., 54 (1985) 2674.
14 A. Hensel, J. Dobbertin, J. E. K. Schawe, A. Boller and C. Schick, J. Thermal Anal., 46 (1996) 935.
15 B. Wunderlich, Macromolecular Physics, Academic Press, New York 1976, Vol. 3.
16 E. Hellmuth and B. Wunderlich, J. Appl. Phys., 36 (1965) 3039.
17 M. Todoki and T. Kawaguchi, J. Polym. Sci., Polym. Phys. Ed., 15 (1977) 1507.
18 I. Okazaki and B. Wunderlich, Macromolecules, 30 (1997) 1758.
19 K. Ishikiriyama and B. Wunderlich, J. Polym. Sci., B, Polym. Phys. Ed., 35 (1997) 1877.